Identification of Volterra Kernels Using Interpolation

József G. Németh, István Kollár, *Fellow, IEEE*, and Johan Schoukens, *Fellow, IEEE*

***Abstract*—This paper presents a new method for the identification of frequency-domain Volterra kernels. Since the nonlinear kernels often play a secondary role compared to the dominant, linear component of the system, it is worth establishing a balance between the degree of liberty of these components and their effect on the overall accuracy of the model. This is necessary in order to reduce the model complexity, hence the required measurement length. Based on the assumption that frequency-domain kernels are locally smooth, the kernel surfaces can be approximated by interpolation techniques, thus reducing the complexity of the model. Similarly to the unreduced (Volterra) model, this smaller model is also i) linear in the unknowns; ii) only locally sensitive to its parameters; and iii) free of structural assumptions about the system. The parameter estimation boils down to solving a linear system of equations in the least-squares (LS) sense. The design of the interpolation scheme is described and the performance of the approximation is analyzed and illustrated by simulation. The algorithm allows a significant saving in measurement time compared to other kernel estimation methods.**

***Index Terms*—B-spline, interpolation, nonlinear system, random multisine, system identification, Volterra kernel, Volterra series.**

I. Introduction

MANY nonlinear systems can be described by a Volterra series [1] and can be well approximated around an operating point by the first few terms of such a series. In this paper, the focus is on the identification of a second-order kernel. The frequency-domain transform of a second-order Volterra series is shown in (3). It is linear in the unknowns ($G^{(1)}(k_1)$, $G^{(2)}(k_1, k_2)$); however, there are many more unknowns than equations obtained from a single measurement. The objective is to reduce the number of necessary measurements.

II. Preliminaries

A. Normalized Random Multisine Excitation Signals

In this paper, a normalized random multisine excitation will be used. Multisine excitation and frequency-domain methods for the identification of linear systems are treated in [2]–[4] and [5]. A random multisine is a broadband, periodic signal

$$u(t) = \sum_{k=-N}^{N} U(k) e^{j2\pi k/N f_{\max} t} \tag{1}$$

with $U(k) = \bar{U}(-k) = |U(k)|e^{j\varphi_k}$, where $f_{\max}$ is the maximum frequency of the excitation signal, and N is the number of frequency components and the phases φ_k are independent, uniformly distributed, random variables on $[0, 2\pi)$, such that $E\{e^{j\varphi_k}\} = 0$. Different random phases result in different realizations of the random multisine. Let $\hat{U}(f) : [0, f_{\max}] \rightarrow \mathbb{R}^+$. If N is varied, then $u(t)$ can be normalized: $|U(k)| = (1/\sqrt{N})\hat{U}((|k|/N) \cdot f_{\max})$, resulting in a *normalized* random multisine. Its time-domain amplitude distribution is asymptotically Gaussian, its root-mean-square (rms) is asymptotically independent from N, whereas its spectral resolution and period length vary in proportion to N

$$T_{\text{period}} = \frac{N}{f_{\max}}. \tag{2}$$

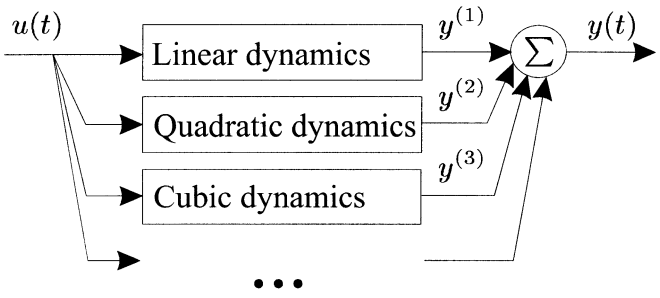

Fig. 1. Linear, quadratic, etc., contributions in the volterra series expansion.

B. Frequency-Domain Truncated Volterra Model

A Volterra series [1] provides a description for dynamic systems in a similar way as the Taylor series does for static input/output relationships, i.e., the system output is split into linear, quadratic, cubic, etc., contributions (see Fig. 1) (N. B. a Volterra series cannot model some nonlinear behaviors, such as hysteresis and chaos, but these are out of scope, here.)

In this paper, the system is restricted to its 1st- and 2nd-order frequency-domain Volterra kernels. The response of this model to a multisine excitation (1) is periodic and can be described by the following Fourier coefficients

$$\begin{aligned} Y(k) =& Y^{(1)}(k) + Y^{(2)}(k) \\ =& G^{(1)}(k)U(k) \\ &+ \sum_{k_1=-N+k}^{N} G^{(2)}(k_1, k-k_1) \\ &\cdot U^{(2)}(k_1, k-k_1), \\ k =& 1, \ldots, N \end{aligned} \tag{3}$$

Manuscript received May 29, 2001; revised May 2, 2002. This work was supported by the Flemish and Hungarian Governments' Bilateral Cooperation Agreement (BIL99/18, TeT Nr. 99/1) and by the Belgian National Fund for Scientific Research, the Flemish Government (GOA-IMMI), and the Belgian government as a part of the Belgian programme on Interuniversity Poles of attraction (IUAP4/2) initiated by the Belgian State, Prime Minister's Office, Science Policy Programming, and the Hungarian National Fund for Scientific Research (OTKA), under contract F033055.

J. G. Németh and I. Kollár are with the Department of Measurement and Information Systems, Budapest University of Technology and Economics, Budapest, Hungary (e-mail: nemeth@mit.bme.hu; kollar@mit.bme.hu)

J. Schoukens is with the Department ELEC, Vrije Universiteit Brussel, Brussels, Belgium (e-mail: johan.schoukens@vub.ac.be).

Digital Object Identifier 10.1109/TIM.2002.803301

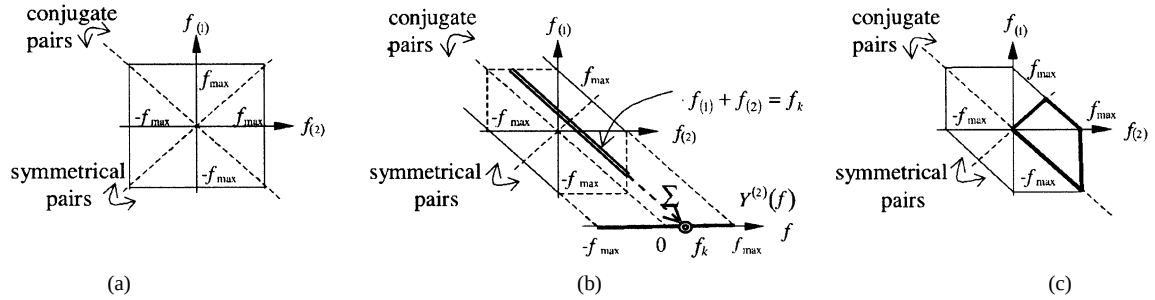

Fig. 2. a) Domain on which the quadratic polyspectrum is different from zero. Symmetrical and complex conjugate pairs. b) Summing the weighted polyspectrum along $f_{(1)} + f_{(2)} = (k/N) \cdot f_{\max} = f_k$ yields $Y^{(2)}(f_k)$. Horizontal, bold segment: Band of observed output. c) Hexagon: Domain on which the kernel can be identified. Trapezoid: Selected nonredundant part of the kernel.

where $U^{(2)}$ is a second-order polyspectrum (the tensor product of two spectra)

$$U^{(2)}(k_1, k_2) = U(k_1) \cdot U(k_2). \tag{4}$$

In these equations,

- $U(k_i)$ is the complex Fourier coefficient of the k_ith harmonic of the input.
- $Y(k)$ is the complex Fourier coefficient of the kth harmonic of the output; $Y^{(1)}(k)$ and $Y^{(2)}(k)$ are the linear and the quadratic contributions, respectively. Only the excited band is observed, hence: $k <= N$.
- $G^{(1)}(k_1)$ and $G^{(2)}(k_1, k_2)$ are samples of the 1st and second-order Volterra kernels, respectively; the index k_i being a substitute for the explicit frequency $(k_i/N) \cdot f_{\max}$. The first-order kernel is a frequency response function (FRF).

The frequency band of the excitation determines the band in which the system characteristics can be identified. This is illustrated for the quadratic kernel in Fig. 2. The quadratic polyspectrum is zero outside the square shown in Fig. 2(a) and contains symmetrical and complex conjugate pairs according to (4). Equation (3) is a weighted sum of (poly)spectrum points, where $G^{(1)}(k_1)$ and $G^{(2)}(k_1, k_2)$ are the weights; the quadratic contributions are illustrated in Fig. 2(b). The kernel can be made symmetrical, too and the domain depicted in Fig. 2(c) can be selected for estimation.

C. Measurement Setup and Operating Point

$U(k)$s and $Y(k)$s are obtained by executing band-limited experiments with the excitation described in (1) and by averaging FFTs of whole periods in steady state. It is important to note that not only the observations are band-limited, but the input to the system, as well. For the sake of simplicity, at first, noise-free observations are assumed. The dc component at the input and the output is considered as an operating point; thus, all terms containing $U(0)$ must be omitted from (3) (where $Y(0)$ is excluded already). This involves that for a pure square-law device, for instance, the identified model will contain nonzero linear components ($G^{(1)}$s) if the operating point is different from 0 ($U(0) \neq 0$).

III. Problem Formulation and New Approach

Equation (3) is a linear problem vis-a-vis the unknowns $G^{(1)}(k_1)$, $G^{(2)}(k_1, k_2)$. By executing a measurement with a single realization of the random multisine, N equations are obtained $k = 1, \ldots, N$. However, the quadratic contributions contain $O\{N^2\}$ complex unknowns. This means that $O\{N\}$ measurements must be accomplished to identify the kernels (each with a different realization of the random multisine).

Meanwhile, if the linear contributions dominate the output power, then this solution wastes measurement time to identify a correction term with full accuracy. Improving the accuracy of the second-order contributions becomes meaningless beyond the point where other disturbing effects (like the noise and the truncated order contributions) start to dominate the output residuals. Hence, a balance should be established between the achievable output accuracy and the degree of liberty of the quadratic terms.

Therefore, in the approach proposed by this paper, $G^{(2)}(k_1, k_2)$ will be considered linearly dependent on each other: the quadratic kernel will be conceived as an interpolated surface, which has linear parameters. Thus, the number of the linear unknowns can be reduced to $O\{N\}$, hence $O\{N^0\}$ realizations of the measurement will be sufficient. The former approach is detailed in Section III-A., while this new approach is introduced in Section III-B.

A. Fundamental Problem Formulation ($O\{N^2\}$ Unknowns)

The linear problem to be solved is slightly different from (3), since

- according to Section II-C, all terms containing $U(0)$ must be omitted;
- the redundant unknowns (symmetrical pairs in $G^{(2)}(k_1, k_2)$) must be eliminated in order to get a full-rank problem.

For each k, the resulting equations (which are not written out explicitly) contain a sum of products [similarly to (3)], which can be written as a scalar product of vectors

$$Y(k) = \mathbf{u}_k^T \cdot \mathbf{g}_k, \; k = 1, \ldots, N \tag{5}$$

where $\mathbf{u}_k$s and $\mathbf{g}_k$s contain the samples of the (poly)spectra and the two kernels, respectively, (the superscript T denoting the transpose, not conjugated). The N equations, which are not coupled, can be assembled into a matrix form

$$\mathbf{y} = \mathbf{U} \cdot \mathbf{g} \tag{6}$$

where $\mathbf{y} = [Y(1), \ldots, Y(N)]$, $\mathbf{g} \in \mathbb{C}^{M \times 1}$ and $\mathbf{U} \in \mathbb{C}^{N \times M}$, with $M = O\{N^2\}$ the number of complex unknowns. $\mathbf{U}$ is a sparse matrix, in each column having a single nonzero entry.

By executing the measurement with more than one realization of the excitation, the obtained $\mathbf{y}$s and $\mathbf{U}$s can be concatenated by rows, yielding

$$\mathbf{y}_{(1\,\text{to}\,R)} = \mathbf{U}_{(1\,\text{to}\,R)} \cdot \mathbf{g} \tag{7}$$

$$\text{with} \quad \mathbf{y}_{(1\,\text{to}\,R)} = [\mathbf{y}_1; \ldots; \mathbf{y}_i; \ldots; \mathbf{y}_R;] \in \mathbb{C}^{R\cdot N\times 1} \tag{8}$$

$$\text{and} \quad \mathbf{U}_{(1\,\text{to}\,R)} = [\mathbf{U}_1; \ldots; \mathbf{U}_i; \ldots; \mathbf{U}_R;] \in \mathbb{C}^{R\cdot N\times M} \tag{9}$$

where R denotes the number of different realizations and the subscript i refers to the ith realization of the measurements. By generating $O\{N\}$ different realizations of the measurements, enough rows could be obtained for solving (7). However, the measurement would take relatively long, unless N is reduced. A similar approach can be found in [6] and [7].

B. New Approach: A Reduced Complexity Model ($O\{N\}$ Unknowns Only)

In order to reduce the number of unknowns, the real and imaginary parts of the quadratic kernel will be sought for on the basis of some interpolation scheme. Since the number of support points (or parameters) for the interpolation scheme can be selected independently from N, the number of unknowns can be scaled down. This technique assumes that the quadratic kernel is locally smooth, i.e., neighboring kernel samples are close to each other in value and this also applies to their variations as well as to the higher order differences.

Without considering the exact choice of interpolation, only its linear property is used

$$\hat{\mathbf{g}}(\mathbf{a}) = \mathbf{P} \cdot \mathbf{a} \tag{10}$$

where $\mathbf{P} \in \mathbb{R}^{M\times L}$ is the interpolation matrix, $\mathbf{a} \in \mathbb{C}^{L\times 1}$ is the parameter vector, with $L = O\{N^0\}$ the number of complex unknowns. Thus, the number of the unknowns may be significantly reduced. Note that (10) implies

$$\text{Re}\,\{\hat{\mathbf{g}}\} = \mathbf{P} \cdot \text{Re}\,\{\mathbf{a}\} \tag{11}$$

$$\text{and} \quad \text{Im}\,\{\hat{\mathbf{g}}\} = \mathbf{P} \cdot \text{Im}\,\{\mathbf{a}\} \tag{12}$$

i.e., the real and imaginary components of the kernel are approximated using the same basis vectors (columns of $\mathbf{P}$). This is accepted for a start to simplify the discussion. The output of the approximate model is

$$\hat{\mathbf{y}}(\mathbf{a}) = \mathbf{U} \cdot \hat{\mathbf{g}}(\mathbf{a}). \tag{13}$$

The output error of the approximate model is

$$\mathbf{h} = \hat{\mathbf{y}} - \mathbf{y}. \tag{14}$$

By adopting the notations of (7)–(9) for the case when several realizations are observed

$$\mathbf{h}_{(1\,\text{to}\,R)} = \hat{\mathbf{y}} - \mathbf{y} \tag{15}$$

$$\text{and} \quad \left\|\mathbf{h}_{(1\,\text{to}\,R)}\right\|_2^2 = \sum_{i=1}^{R} \|\mathbf{h}_i\|_2^2. \tag{16}$$

The performance function will be the mean-square output error

$$MSE\,(\mathbf{a};\mathbf{P}) = E_\varphi\,\{\|\mathbf{h}\|\}\,|_{R=1} \tag{17}$$

where the statistical expectation is taken with respect to all realizations of φ (see Section II-A). $MSE(\mathbf{a})$ is a quadratic function of $\mathbf{a}$ and is parameterized by $\mathbf{P}$. The optimal parameter setting is the one yielding the least-mean-square output error (using a given $\mathbf{P}$)

$$\alpha = \arg\min_{\mathbf{a}} MSE\,(\mathbf{a})\,. \tag{18}$$

To approximate α, the following equation may be solved in the LS sense

$$\mathbf{y}_{(1\,\text{to}\,R)} = \left(\mathbf{U}_{(1\,\text{to}\,R)} \cdot \mathbf{P}\right) \cdot \mathbf{a}. \tag{19}$$

The resulting $\mathbf{a} = \alpha$ minimizes $(1/R)\|\mathbf{h}_{(1\,\text{to}\,R)}\|_2^2$ for the realizations involved in the specific experiment. Since $(1/R)\|\mathbf{h}_{(1\,\text{to}\,R)}\|_2^2$ converges to MSE as $R \to \infty$, it can be proved that $\hat{\alpha}$ is an asymptotically unbiased and weakly consistent estimate of α

$$\forall \varepsilon > 0 : \lim_{R\to\text{inf}} \text{Prob}\,(|\hat{\alpha}(R) - \alpha| > \varepsilon) = 0. \tag{20}$$

IV. Algorithm

A. Steps of the Identification Process

1. Select the operation point and the desired excitation class (rms, $f_{\max}$, etc. ; see Section II-A). The approximation will be optimal for the specified magnitude spectrum and time-domain amplitude distribution.

2. Design $\mathbf{P}$ (see Section IV-B).

3. Select N and R (i.e., the number of harmonics and the number of realizations) so that the equation-to-unknown ratio of (19) be $R\cdot(N/L) > 1$. The necessary ratio also depends on the noise level and the higher order nonlinear contributions. Then generate a multisine to start the measurements. The duration of the measurements is equal to

$$T_{\text{meas}} = p \cdot \frac{R \cdot N}{f_{\max}} \tag{21}$$

where p is the number of periods measured with each realization. It is necessary to wait several periods to achieve steady state. Additional periods can be measured to filter the additive noise by averaging the FFTs. The higher order nonlinear contributions are periodic; hence, these are not filtered with the noise. On the other hand, these can be averaged by increasing R and N. It is advised to carry out additional realizations of the measurements (e.g., $R_{\text{test}} = R/4$) to collect observations as test data for the assessment of the later estimate.

4. When the data are available, solve (19) in the LS sense to obtain $\hat{\alpha}$, but do not use the test data for this estimation.

5. Estimate $MSE(\hat{\alpha};\mathbf{P})$ by using the test data: $\hat{MSE}(\hat{\alpha};\mathbf{P},\mathbf{U}_{\text{test}}) = (1/R_{\text{test}})\|\mathbf{h}(\hat{\alpha};\mathbf{P},\mathbf{U}_{\text{test}})\|_2^2$. If $\hat{MSE}(\hat{\alpha})$ is satisfactory, then the procedure may be finished, or the result might be improved by including the 'test data' in the estimation of α. If $\hat{MSE}(\hat{\alpha})$ is not satisfactory, then further iterations are necessary through steps 3–5 (keeping P) or 2–5. (The recursive least-squares solution is out of the scope, here. See [7]).

B. Design of the Interpolation Scheme (Matrix P)

Interpolation by B-splines [8] is used because it is i) locally smooth; ii) only locally sensitive to the parameters; and iii) it can be applied to arbitrary dimensions by tensor product extension. The two-dimensional extension is as follows.

$$\hat{f}(x,y) = \sum_{i,j=1}^{n,m} a_{i,j} B_{i,j}^{(2)}(x,y) = \sum_{l=1}^{n\cdot m} a_l B_l^{(2)}(x,y) \quad (22)$$

$$\text{where} \quad B_{i,j}^{(2)}(x,y) = B_i(x) \cdot B_j(y). \quad (23)$$

$\{B_i(x)\}_1^n$ is a "horizontal" B-spline basis, whereas $\{B_j(y)\}_1^m$ is a "vertical" B-spline basis. If values of $\hat{f}(x,y)$ are arranged in a column vector $\hat{\mathbf{g}}$ and $\{B_{i,j}^{(2)}(x,y)\}_1^{m\cdot n}$ are arranged likewise into the columns of a matrix P, then (10) is obtained formally. (The difference is that $\hat{\mathbf{g}}$ in (10) includes the linear kernel, too, which is not reduced by interpolation).

Two alternatives are obvious in selecting the directions for the horizontal and the vertical axes

1) parallel to the frequency axes of the quadratic kernel;
2) parallel to the complex conjugation axis and the symmetry axis of the quadratic kernel, respectively.

Only the latter option is analyzed here (see Fig. 4). To avoid unnecessary boundary effects, first, a basis must be designed over the redundant kernel area; then, the redundant parameters must be eliminated by taking into account the symmetries of the quadratic kernel (see Figs. 3–4). Finally, the basis functions must be 'clipped' to the nonredundant kernel area.

Since the real part of the kernel is symmetrical to $f_{(1)}+f_{(2)} = 0$, whereas the imaginary part is anti-symmetrical to it, different basis vectors should be used for the two surfaces. If this choice is taken, then (11)–(12) are replaced by $\mathrm{Re}\{\hat{\mathbf{g}}\} = \mathbf{P}_{\mathrm{sym}} \cdot \mathbf{a}_{\mathrm{Re}}$ and $\mathrm{Im}\{\hat{\mathbf{g}}\} = \mathbf{P}_{\mathrm{anti-sym}} \cdot \mathbf{a}_{\mathrm{Im}}$ and the following equation must be solved in the LS sense, instead of (19):

$$\begin{bmatrix} \mathrm{Re}\{\mathbf{y}\} \\ \mathrm{Im}\{\mathbf{y}\} \end{bmatrix}_{(1\,\mathrm{to}\,R)} = \begin{bmatrix} \mathrm{Re}\{\mathbf{U}\} & -\mathrm{Im}\{\mathbf{U}\} \\ \mathrm{Im}\{\mathbf{U}\} & \mathrm{Re}\{\mathbf{U}\} \end{bmatrix}_{(1\,\mathrm{to}\,R)} \cdot \begin{bmatrix} \mathbf{P}_{\mathrm{sym}} & 0 \\ 0 & \mathbf{P}_{\mathrm{anti-sym}} \end{bmatrix} \cdot \begin{bmatrix} \mathbf{a}_{\mathrm{Re}} \\ \mathbf{a}_{\mathrm{Im}} \end{bmatrix} \quad (24)$$

where all values are real. The total number of real-valued parameters shall be denoted by L_{Re} (sum of lengths of a_{Re} and a_{Im}). The equation-to-unknown ratio in (24) is $2 \cdot R \cdot N / L_{\mathrm{Re}}$.

At interpolation boundaries, the constraints are fewer. When the B-splines are constructed, this is taken into account, which solves the problem for the boundaries of the basis (see the rectangle in Fig. 4). However, these boundaries do not match the boundaries of the excited domain of the kernel at $f_{(1)} = f_{\max}$ and $f_{(2)} = f_{\max}$. Consequently, here the degree of liberty of the interpolation is too high. This will set back the performance of the estimation.

C. Computational Complexity

The computational complexity is dominated by the solution of the least-squares problem. In the simulations, Gaussian elimination was used implying $2 \cdot R \cdot N \cdot L_{\mathrm{Re}}^2$ flops.

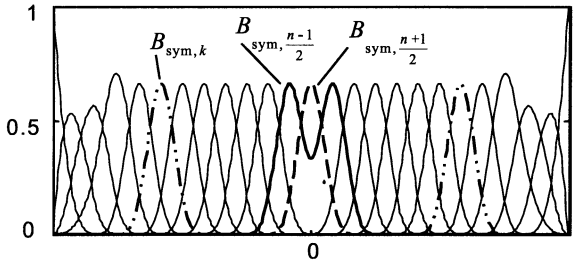

Fig. 3. Symmetrical basis obtained from cubic B-splines (with uniform knot-placement and not-a-knot boundary condition): $B_{\mathrm{sym},k} = B_k + B_{n-k}, k = 1, \ldots, (n-1/2)$ and $B_{\mathrm{sym},(n+1)/2} = B_{(n+1)/2}$.

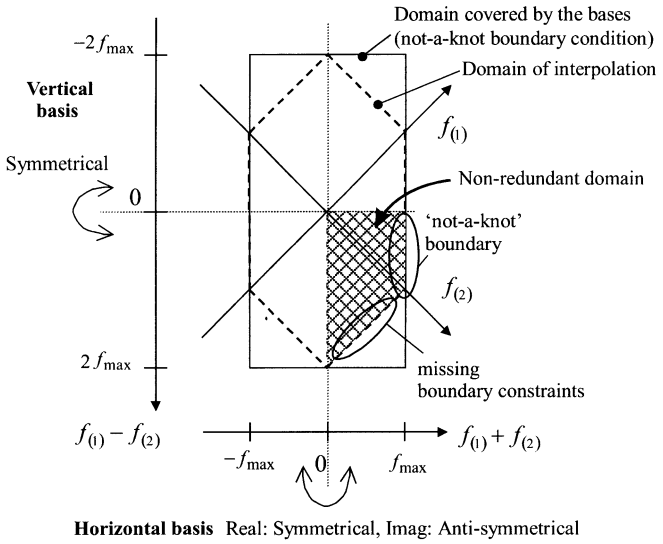

Fig. 4. The bases (for the real and imaginary parts of the quadratic kernel) are defined by the tensor product of the horizontal and the vertical bases.

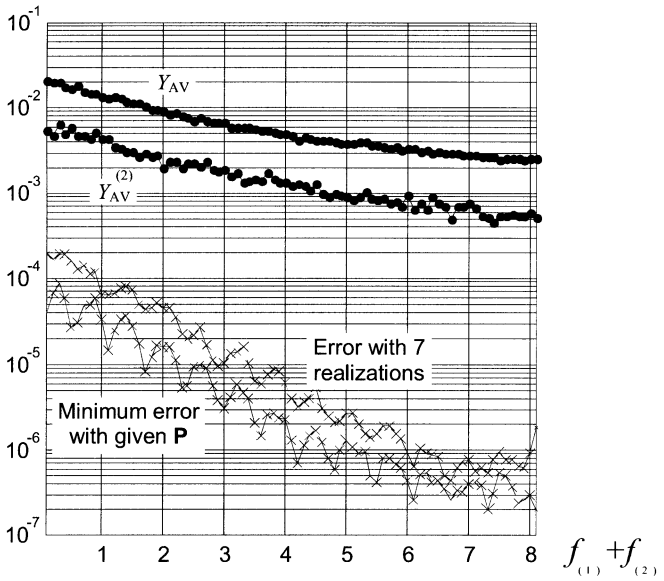

Fig. 5. Frequency components of the root-mean-square error as R increases. With seven realizations (1.5 equation/unknown ratio), the error is close to the attainable minimum.

TABLE I
FOUR CASES: INTERPOLATION SCHEMES AND NUMBER OF REALIZATIONS USED

# of quadratic kernel param. $L_{\mathrm{Re}} - 2 \cdot N$	cubic	5th order	# of realizations R	Equation-to-unknown ratio $2 \cdot R \cdot N / L_{\mathrm{Re}}$
573	$\mathbf{P}_1$	$\mathbf{P}_2$	7	1.54
1179	$\mathbf{P}_3$	$\mathbf{P}_4$	12	1.45

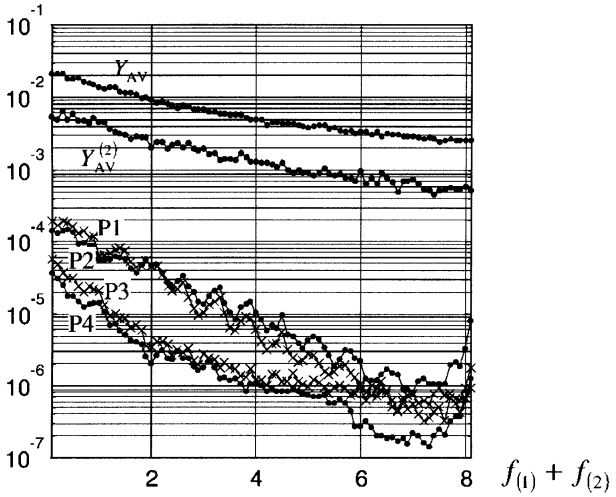

Fig. 6. Frequency components of the root-mean-square error (estimated using 30 independent realizations). P1,P3: cubic splines used, P2,P4: 5th order splines, P1,P2: 7 realizations, P3,P4: 12 realizations.

V. MINIMIZATION OF DISTURBING EFFECTS

Suppose that the physical system being identified can be described by a Volterra series; then some of the following effects may dominate the $MSE(\hat{\alpha}; \mathbf{P})$:

1) *Limited capability of the interpolation scheme to approximate the optimal surface.* The model set is reduced by (10). Since in general $\hat{\mathbf{g}} \notin range(\mathbf{P})$, an approximation error is necessarily present, which depends on $\mathbf{P}$ and the system. The larger the number of parameters (L_{Re}) the smaller this error.
2) *Variance of the LS solution.* $MSE(\mathbf{a}, \mathbf{P})$ has one single minimum: $MSE(\alpha, \mathbf{P})$; Since $\hat{\alpha} \neq \alpha$, this introduces an additional approximation error. The larger the equation-to-parameter ratio ($2 \cdot R \cdot N / L_{\mathrm{Re}}$), the smaller this error.
3) *Observation noise*. Zero-mean, uncorrelated, additive, output noise introduces no additional bias into α, but increases its variance. Noise in the input observations always introduces some bias, too. The stochastic effects of noise can be filtered out by averaging integer periods with each realization.
4) *Convergence of the Volterra series that describes the true system.* Higher order nonlinear contributions have similar stochastic effects as additive, possibly correlated, output noise. (N.B. As far as systematic contributions are concerned, in [4] and [5] it is shown that even-order nonlinear contributions do not bias the linear FRF estimate, when a linear model is being identified, whereas odd-order contributions do. It also follows, that the output error that is due to the approximation of the quadratic kernel does not introduce a bias in the linear kernel estimate).
5) If an infinite Volterra series can only describe the physical system but approximately, then this presets the lower bound for the approximation error.

In order to collect and extract the maximum information about the system based on a limited length of measurements, all the enumerated effects should be kept in balance by selecting the adequate parameters for the experiments and the identification. The main advantage of the proposed method is in fact that it allows this optimization and reduces the required measurement length.

VI. SIMULATIONS

A. The Simulated System

In this section, simulations are provided using the system

$$\dot{y}(t) + a \cdot y(t) = b \cdot u(t) + c \cdot u^2(t) \tag{25}$$

where $a = b = c = 2\pi$. The operating point is $U(0) = 0$. The rms of the excitation is 0.25 V, whereas its bandwidth is $f_{\max} = 8.1$ Hz. Throughout the simulations $N = 81$, harmonics are applied and the magnitude spectrum is flat. The observations are noiseless and the system does not produce higher order nonlinear contributions; thus, points one and two of the previous section are illustrated in the following.

B. Variance of the Least-Squares Solution

By increasing the number of realizations (R), the MSE must decrease (see point 2 in the previous section). In Fig. 5, Y_{av} is the rms of the output of the system, Y_{av}^2 is the quadratic component of Y_{av} (which cannot be observed in a physical measurement), whereas the lower two curves show the rms error at each frequency, when using 7, and 12 realizations, respectively. (In both cases, the residual curves were estimated by using 30 realizations of the experiment that were reserved for validation). The lower curve can be considered as the floor of the error that can be attained with the current interpolation scheme. The convergence is rapid, since with seven realizations the error is close to this reference curve.

C. Performance of Several Different Interpolation Schemes

The performance of four interpolation schemes will be compared and the notation adopted in Table I will be used. For the interpolation schemes that have fewer parameters, fewer observations are used for the parameter estimation.

In Fig. 6, the lower curves are the mean-square error components for each frequency. Curves P1, P2, P3, and P4 must be compared to $Y_{\mathrm{av}}^{(2)}$ since they mostly result from the error

of the quadratic kernel. Near $f_{(1)} + f_{(2)} = 0$ the approximation performs worse due to the steep variation of the kernel surface in this region. Near $f_{\max} = 8.1$ Hz the error grows rapidly due to boundary effects (Figs. 4 and 6). The curves are in agreement with the expectations. Namely, fifth-order splines can better follow the variations of the kernel surface, but they are also more vulnerable to boundary effects, since the basis functions have larger support. These effects are smaller when the number of the parameters is high.

VII. Conclusion

If a linear model had been identified in the simulations, then the output error would be the same as $Y_{\text{av}}^{(2)}$ (Fig. 6) since the second-order contributions do not bias the linear FRF [4], [5]. This illustrates the efficiency of the quadratic models that were obtained: the error curve P1 is 30–45 dB below $Y_{\text{av}}^{(2)}$. What is gained by the new Volterra kernel estimation approach? Taking the just mentioned case, the saving in measurement time is a ratio of $N/R = 13(!)$ compared to the solution of the nonparametric problem setting as described in Section III-A.

The proposed approach has recently been implemented to third-order Volterra models [9], too, where the benefits are even greater.

References

[1] M. Schetzen, *The Volterra and Wiener Theories of Nonlinear Systems*: Wiley-Interscience, 1980.

[2] J. Schoukens and R. Pintelon, *Identification of Linear Systems: A Practical Guide to Accurate Modeling*. New York: Pergamon, 1991.

[3] K. R. Godfrey, *Perturbation Signals for System Identification*. Englewood Cliffs, NJ: Prentice-Hall, 1993.

[4] R. Pintelon and J. Schoukens, *System Identification: A Frequency Domain Approach*. Piscataway, NJ: IEEE Press, 2001.

[5] J. Schoukens, T. Dobrowiecki, and R. Pintelon, "Identification of linear systems in the presence of nonlinear distortions. a frequency domain approach," *IEEE Trans. Automat. Control*, vol. 43, no. 2, 1998.

[6] K. I. Kim and E. J. Powers, "A digital method of modeling quadratically nonlinear systems with a general random input," *IEEE Trans. Acoust. Speech Signal Process.*, vol. 36, pp. 1758–1769, Nov. 1988.

[7] S. W. Nam and E. J. Powers, "Application of higher order spectral analysis to cubically nonlinear system identification," *IEEE Trans. Signal Processing*, vol. 42, pp. 1746–1765, July 1994.

[8] C. de Boor, *A Practical Guide to Splines*: Springer, 1978.

[9] J. Nemeth and J. Schoukens, "Efficient identification of third order volterra models using interpolation techniques," in *IEEE Instrum. Meas. Technol. Conf.*, Anchorage, AK, May 2002.

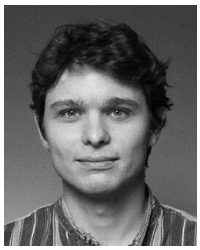

József G. Németh was born in Budapest, Hungary, in 1973. He received the M.S. degree in electrical engineering from the Technical University of Budapest, Budapest, in 1998. He is currently pursuing the Ph.D. degree at the Department of Measurement and Information Systems, Technical University of Budapest.

His main research interests are frequency domain system identification and DSP applications.

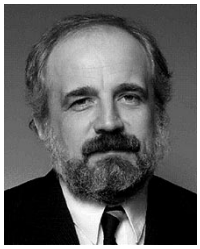

István Kollár (F'97) was born in Budapest, Hungary, in 1954. He graduated in 1977 in electrical engineering from the Technical University of Budapest. In 1985, he received the degree "Candidate of Sciences" (the equivalent of Ph.D.) and in 1997 the degree "Doctor of the Academy," both from the Hungarian Academy of Sciences, Budapest.

He is Professor of electrical engineering at the Budapest University of Technology and Economics, Budapest. From 1989 to 1990, he was a Visiting Scientist at the Vrije Universiteit Brussel, Brussels, Belgium. From 1993 to 1995, he was a Fulbright Scholar and Visiting Associate Professor with the Department of Electrical Engineering, Stanford University, Stanford, CA. His research interests span the areas of digital and analog signal processing, measurement theory and system identification. He has published about 90 scientific papers and he is co-author of the book *Technology of Electrical Measurements* (Schnell L., ed; New York: Wiley, 1993). He authored the Frequency Domain System Identification Toolbox for Matlab.

Dr. Kollár is an active member of EUPAS.

Johan Schoukens (F'97) received the degree of engineer in 1980, the degree of doctor in applied sciences in 1985, and geaggregeerde voor het hoger onderwijs in 1992, all from the Vrije Universiteit Brussel (VUB), Brussels, Belgium.

He is presently a Professor with the VUB. The prime factors of his research are in the field of system identification for linear and nonlinear systems and growing tomatos in a greenhouse. He is member of the Coppighaerdt.